Computers and Electronics in Agriculture 176 (2020) 105633

Contents lists available at ScienceDirect

Computers and Electronics in Agriculture

journal homepage: www.elsevier.com/locate/compag

Original papers

Supplanting missing climatic inputs in classical and random forest models for estimating reference evapotranspiration in humid coastal areas of Iran

Sepideh Karimi[a], Jalal Shiri[a,b,*], Pau Marti[c]

[a] Water Engineering Department, Faculty of Agriculture, University of Tabriz, Iran
[b] Center of Excellence in Hydroinformatics, Faculty of Civil Engineering, University of Tabriz, Iran
[c] Àrea d'Enginyeria Agroforestal, Universitat de les Illes Balears, c/Ctra Valldemossa km 7.5, 07022 Palma, Spain

ARTICLE INFO

Keywords:
Calibration
Cluster analysis
Correlation matrix
Data scarcity
Local models

ABSTRACT

Although evapotranspiration might not be a limiting factor for water consumption in humid regions, it is a very important parameter in irrigation scheduling and agricultural water management in those regions, and should be estimated with high accuracy. The reference evapotranspiration (ET_o) concept is a way for retrieving the actual crop water requirements using a crop coefficient. The standard procedure for determining ET_o values in literature is the Penman-FAO-Monteith (PFM) equation, which needs considerable meteorological inputs. In practice, when all necessary data of PFM are not available, the consideration of estimated meteorological inputs for this equation might be a suitable approach for deriving accurate ET_o values. Further, the empirical ET_o equations and machine learning techniques relying on fewer meteorological variables are usually employed as alternatives to the PFM equation. The present paper aimed at assessing the effect of considering calculated missing meteorological variables on the performance accuracy of the standard PFM and some commonly used empirical equations using daily data from six humid coastal locations in Iran covering a period of 10 years. Moreover, the machine learning bootstrap aggregating-based random forest (RF) technique was applied under the same conditions. Based on the obtained results, when replacing missing inputs by calculated ones, the combination-based models (relying on estimated wind speed values) provided the most accurate results, while using estimated solar radiation values reduced the model's performance accuracy.

1. Introduction

Most of the precipitation amount received by the ground surface is returned to the atmosphere by the evapotranspiration process (combined water loss due to the evaporation from the soil surface and crop transpiration). Precise estimation of evapotranspiration (*ET*) is very important at any region, as it affects the hydrologic cycle that roles all hydrologic and near ground terrestrial phenomena. *ET* is an important indicator in water resources planning and management, irrigation scheduling, land drainage implementation, groundwater studies, drought analysis, environmental analysis and agricultural water management. Despite water availability and crop type, meteorological factors (e.g. air temperature, humidity, solar radiation and wind speed) have considerable effects on *ET* values under different climatologic conditions. Regions with arid climates and limited water resources show higher magnitudes of *ET* records especially during the warm seasons, thus usually exhibit negative water budget during specific time periods. Hence, *ET* is a crucial factor in such regions, and should be accurately determined for a through water loss analysis. Humid regions, on the other hand, receive considerable amounts of precipitation during a year that can compensate the water losses due to *ET* process, although water balance in the summer, when evapotranspiration amount exceeds rainfall amount, can be negative. Although *ET* might not be a limiting factor for water using in such regions, agricultural activities (especially in irrigated cultivations) need an accurate *ET* value for any water-related activity in the farm and hydrologic basin scales. Moreover, this parameter would be a crucial input for establishing any hydrologic model in humid/arid regions. Therefore, it is necessary to have accurate in-situ estimations of *ET* in different locations under any climatic context. The main approaches of *ET* measurement are e.g. water balance method (Guitjens, 1982), water vapor mass flux transfer method (Harbeck, 1962) or lysimeter installation that imply all influential parameters on *ET* (crop type and age, soil moisture, meteorological conditions, etc). However, these approaches are time consuming and expensive, limiting their applicability. Another possibility for determining actual *ET* values is to apply the concept of reference *ET*.

* Corresponding author at: Water Engineering Department, Faculty of Agriculture, University of Tabriz, Iran.
E-mail address: j_shiri2005@yahoo.com (J. Shiri).

https://doi.org/10.1016/j.compag.2020.105633
Received 16 April 2020; Received in revised form 8 July 2020; Accepted 8 July 2020

Reference evapotranspiration (ET_o) represents the ET amount of a green well-watered hypothetical canopy (grass) with a height of 12 cm, aerodynamic resistance of 70 s/m and an albedo coefficient of 0.23 (Allen et al., 1998). Using this definition, ET_o can be calculated from meteorological variables through physics-based or empirical equations.

According to the FAO recommendation (Allen et al., 1998), the physically-based Penman-FAO-Monteith equation (PFM) can be applied for calculating the ET_o values when measurements of this parameter are not available. Among the major advantages of this equation are its physical basis, its worldwide validation, as well as not requiring local preliminary calibration. On the other hand, the high input requirement is a major downside of PFM equation. Furthermore, other physically-based equations, e.g. Kimberly-Penman (KP) (Wright and Jensen, 1972), can be used for computing alfalfa-reference ET (ET_r). However, the values obtained by this equation should be adjusted to provide the reference grass ET values (ET_o) in order to assess its performance accuracy against the standard PFM equation. Therefore, adopting the original PFM equation using estimated meteorological variables (in case of data scarcity) or applying the empirical equations relying on fewer input variables are common and valid practices worldwide. However, as the basis of such kinds of studies is empirical, a priori (before conducting the study) it is difficult to decide if a simpler equation is preferable to more complex models relying on calculated inputs. Stockle et al. (2004) utilized the weather generator ClimGen for estimating solar radiation and humidity data using 2–5 years daily data and concluded that applying PFM with estimated meteorological variables provided poor to acceptable results for daily values, while their performances using weekly values were suitable. Gong et al. (2006) analyzed the sensitivity of PFM equation to meteorological variables in China and stated that the relative humidity was the most influential variable, followed by the solar radiation, air temperature and wind speed. Popova et al. (2006) calculated the PFM ET_o values with estimated meteorological variables using 15 year observations of four weather stations in Bulgaria. Jabloun and Sahli (2008) applied PFM equation under full and limited data conditions in Tunisia and concluded that it provided promising outcomes in both states. Landeras et al. (2008) evaluated various scenarios of PFM equation applications with estimated solar radiation and relative humidity parameters in Spain and found that the error magnitudes when using estimated solar radiation values were higher than those of the relative humidity. Sentelhas et al. (2010) examined the PFM performance accuracy with full and limited input variables using five years data from Canada. Their results showed that wind speed and relative humidity had little effect on the PFM performance, while when solar radiation data were missing, PFM accuracy decreased considerably. Cordova et al. (2015) evaluated PFM equation with limited data using meteorological variables of two high-elevation weather stations in Ecuador and found that using estimated wind speed values had lower impact than the estimated solar radiation values on final PFM performance accuracy. These studies used a method relying on temperature range (as will be explained later) for solar radiation estimation and regional averaging (average of corresponding events of nearby stations) for wind speed estimation. Djaman et al. (2016) assessed the PFM capability under limited data conditions using 14 years data from eight Sahelian sites. Based on their results, estimating solar radiation using temperature range produced reliable ET_o outcomes for the studied regions. They also reported that estimating missing wind speed values by utilizing local long term values of this parameter provided promising results than using the recommended default value suggested by the FAO (wind speed = 2 m/s). Similar statements have been already presented by Rojas and Sheffield (2013). Shiri (2017) applied PFM equation for arid regions with limited observed meteorological parameters and stated that the PFM equation that used the estimated solar radiation values (using temperature range method) provided the most accurate results. The reviewed literature showed that estimation of one or more meteorological variables affects the performance accuracy of PFM model when compared to the situations where all data are available. The effect is more marked depending on the missing parameter and its significance on the ET process in the studied climatic context.

As an alternative to the PFM model, either empirical equations or heuristic data driven approaches, relying on limited meteorological parameters, might be used. Among the different existing equation alternatives in the literature, some equations have been applied and assessed widely under different climatic contexts, viz., temperature-based Hargreaves-Samani equation (HR) (Hargreaves and Samani, 1982) and radiation-based Priestley-Taylor (PT) (Priestley and Taylor, 1972), Makkink (MK) (Makkink, 1957) and Turc (TU) (Turc, 1961) equations. These equations differ in the way they select the input variables (meteorological factors). Trajkovic and Kolakovic (2009) compared different temperature-based and radiation-based equations against the standard PFM model (monthly time step) in some humid stations and introduced the Turc model as the most accurate approach of ET_o estimating in humid climates. Tabari (2010) evaluated HR, TU, MK and PT equations under four climatic conditions of Iran and found that the TU equation provided the most accurate results in cold humid and arid climates, whereas the HR produced the best results in warm humid and semi-arid climates. Tabari et al. (2013) applied some empirical ET_o equations under humid conditions of Iran and stated that the radiation-based models provided the most accurate estimates of the target PFM-ET_o values. Gao et al. (2017) assessed the performance of some empirical equations in different regions and concluded that the MK equation outperformed the other radiation-based as well as temperature-based equations in humid locations of U.S.A. Bourletsikas et al. (2018) evaluated 24 ET_o estimation equations for a grass-covered ground in a Mediterranean evergreen forest in Greece and stated that the temperature-based HR equation outperformed the other applied equations. Farzanpour et al. (2019) compared 20 empirical ET_o equations in a semi-arid region of Iran and found that the temperature-based and radiation-based equations have a similar performance in those locations.

Regarding machine learning approaches, a wide range of studies have been performed adopting different modeling scenarios under different climatic conditions. A complete review of machine learning applications for ET estimation is beyond the scope of this paper, thus some most relevant studies will be reviewed here. Torres et al. (2011) applied multivariate relevance vector machine technique for forecasting ET_o values by limited input variables in Utah State and found that this technique can be used in ET_o forecasting issues with limited data. Tabari et al. (2012) introduced data driven support vector machine and neuro-fuzzy techniques as suitable candidates for ET_o estimating with limited input variables. Abdullah et al. (2015) made a sensitivity analysis through extreme learning machine for identifying the most influential parameters on ET_o in Iraq stations. Based on their report, the most effective parameter differs among the stations and during the years. Feng et al. (2016) compared different neural-networks methodologies for estimating ET_o values of humid regions and reported that the models constructed with temperature and radiation data provided the most accurate results in those regions. Feng et al. (2017) employed neural network and random forest (RF) in simulating daily ET_o values utilizing the 6-years meteorological records of two weather sites in China and stated that the RF model slightly outperformed the neural network. Karimi et al. (2017) evaluated gene expression programming and support vector machine techniques in estimating daily ET_o values of humid regions using local and exogenous data supply strategies and found that both the techniques gave promising outcomes when the available data are limited and should be obtained from other (similar) locations. Shiri (2018) introduced a coupled wavelet-random forest methodology for improving the performance of mass-transfer based ET_o equations in arid and hyper arid regions. Huang et al. (2019) compared CatBoost, RF and support vector machine techniques in estimating daily ET_o values using data from five humid locations in South China under full and limited data availability conditions. Their results showed that

when all necessary data are available, the CatBoost techniques surpassed the RF and support vector machine models, while with data scarcity, support vector machine and RF provided promising results. Wang et al. (2019) applied RF and genetic programming to estimate ET_o in China and confirmed the capabilities of both the techniques in simulating ET_o values under full and limited data conditions.

As a first step of the present study, Shiri (2017) evaluated several equations and genetic programming based alternatives in inland arid and hyper-arid regions of Iran under scenarios of full and limited data availability. Nevertheless, this analysis has not been carried out in coastal humid regions so far. In the present research, the performance of the commonly used empirical ET_o equations has been evaluated in a humid coastal region of Iran, using a similar framework. As mentioned, air humidity and evapotranspiration are the most important meteorological factors in coastal locations. A comparison was also made between those models and a machine learning bootstrap aggregating-based random forest (RF) technique based on the same input combinations.

2. Materials and methods

2.1. Used data

Daily meteorological records of six automated weather stations located in the Northern coastal region of Iran covering a period of 10 years (2008–2017) were used in the present study to assess the presented methodology. The dataset consisted of maximum (T_{max}) and minimum (T_{min}) air temperature, relative humidity (R_H), global incoming solar radiation (R_S), wind speed (S_W) and rainfall amount (P). Table 1 summarizes the general information of the studied locations. Among the studied sites, Lahijan has the highest elevation (34.2 m.a.s.l), while Astara is located at the lowest elevation (−21.1 m.a.s.l). The values of the aridity index (I_A) (UNEP, 1997) have been given in Table 1. This index denotes the ratios between the annual precipitation and annual ET_o values at any specified location. The regions with $I_A > 0.65$ are classified as humid locations. Based on the I_A values presented in Table 1, the studied stations in the present research are classified as humid sites. All available data were thoroughly screened and checked for fixing any possible inconsistency.

Table 1
Summary of the studied weather stations.

Station	Latitude (°N)	Longitude (°E)	Elevation (m)	I_A
Amol	36.47	52.38	23.70	0.97
Astara	38.37	48.85	−21.10	1.68
Lahijan	37.19	50.02	34.20	2.18
Ramsar	36.90	50.68	−20.00	1.86
Rasht	37.32	49.62	−8.60	1.62
Sari	36.54	52.99	23.00	0.71

Mean and coefficient of variation (in brackets)values of used data

	T_A(°C)	R_H (%)	R_S (MJ/m^2day)	S_W (m/s)	ET_o (mm/day)
Amol	17.29 (0.44)	81.58 (0.08)	15.94 (0.37)	1.36 (0.58)	2.88 (0.51)
Astara	15.85 (0.49)	80.17 (0.13)	16.14 (0.43)	1.09 (0.59)	2.79 (0.59)
Lahijan	17.22 (0.45)	79.29 (0.15)	15.56 (0.40)	1.20 (0.63)	2.81 (0.56)
Ramsar	17.14 (0.43)	80.66 (0.10)	15.16 (0.41)	1.30 (0.59)	2.72 (0.55)
Rasht	16.56 (0.46)	82.75 (0.12)	15.53 (0.43)	1.14 (0.60)	2.78 (0.58)
Sari	17.91 (0.44)	78.51 (0.12)	15.60 (0.43)	0.95 (0.63)	2.89 (0.56)

2.2. Formulation of ET_o

Table 2 summarizes the applied ET_o equations. As mentioned, the standard PFM equation was used as the benchmark model for calibrating and evaluating other applied equations and the machine learning models. In the present paper, three kinds of equations were assessed against the standard PFM model, e.g. temperature-based Hargreaves-Samani (HR), radiation-based Priestley-Taylor (PT), Makkink (MK) and Turc (TU) equations and the physically-based Kimberly-Penman (KP) equation of reference alfalfa ET (ET_r). Temperature-based HR equation is accepted to provide suitable estimations of ET_o under different climatologic contexts for daily or monthly periods (Shiri, 2017). This equation needs only air temperature records for estimating ET_o. The radiation-based PT, MK and TU equations consider air temperature and solar radiation records (except TU which requires additionally relative humidity data). Based on climatic regimes of different regions, these models have been proven as acceptable approaches for ET_o estimations. Finally, the physically-based KP equation that calculates the alfalfa reference crop ET might be considered as a suitable tool for partitioning the effects of energy balance and aerodynamic components in evapotranspiration formation. KP considers a wind function defined as $W_f = a_w + b_w W_S$ that depends on both wind speed and the day of year (day numbers of calendar).

Following the Allen et al. (1998) recommendation, the applied empirical equations were calibrated against the standard PFM model using a regression equation (at 95% confidence level) as:

$$ET_o^{PFM} = a * ET_o^{\mathrm{mod}\ el} + b \quad (1)$$

where, ET_o^{PFM} and ET_o^{model} represent the ET_o values obtained by the benchmark PFM and other applied equations, respectively. With this calibration the comparison of empirical equations with random forest models will be fairer, because the latter ones require local patterns for their development. Shiri et al. (2014) argued that different calibration procedures, e.g. linear, nonlinear (power, etc) can be used to calibrate the empirical equations against the standard PFM model under various climatic contexts; from which the linear equation provide most accurate results among others.

2.3. Random forest (RF)

As a tree-based group approach, random forest (RF) handles high-dimension regression issues, where the forest's growth is based on numerous connected trees (Breiman, 2001; Chen et al., 2007; Karimi et al., 2018). The ultimate solution is the consequence of bagging procedure, e.g. averaging the output after fitting the single trees in ensemble (Shiri, 2018). The bias of the bagged and single trees is similar, but the variance is dependent on the correlation values among the trees (Hastie et al., 2009). The regression-based RFs formation is started by growing trees on the basis of random vector, Θ so that tree estimator h (X,Θ) may get numerical values. The mean-squared generalization error of any specified numerical predictor h(X) can be written as (Breiman, 2001):

$$E_{X,Y} = (Y - h(X))^2 \quad (2)$$

The formation of RF predictor is conducted by taking an average over j of the single trees. Here, the following theorems stand in this regrad:

Theorem 1.. By increasing the forest's tree number, the error will be:

$$E_{X,Y}(Yav_j h(X, \Theta_j))^2 \rightarrow E_{X,Y}(Y - E_\Theta h(X, \Theta))^2 \quad (3)$$

Also, the average generalization error of a tree is (Breiman, 2001):

$$PE_*(tree) = E_\Theta E_{X,Y}(Y - h(X, \Theta))^2 \quad (4)$$

Theorem 2.. Let's suppose that EY = Ex h(X,Θ) for all Θ, then:

Table 2
Mathematical formulations of the employed equations.

NAME	ABBREVIATION	Meteorological inputs	missing input parameter	expression
ET_o equations applied with full data (first scenario)				
Penman-FAO-Monteith	PFM	T_{mean}, R_S, S_W, R_H	–	$ET_o = \frac{0.408\Delta(R_n - G) + \gamma\frac{900}{T_{mean}+273}SW(e_s - e_a)}{\Delta + \gamma(1 + 0.34S_W)}$
Kimberly-Penman	KP	T_{mean}, R_S, S_W, R_H	–	$\lambda ET_r = \frac{\Delta}{\Delta+\gamma}(R_n - G) + \frac{\gamma}{\Delta+\gamma}6.43W_f(e_S - e_a)$
Hargreaves-Samani	HR	T_{mean}, $T_{\max}$, $T_{\min}$	–	$ET_0 = 0.0023R_a(T_{mean} + 17.8)\sqrt{T_{\max} - T_{\min}}$
Priestly-Taylor	PT	$T_{\max}$, $T_{\min}$, T_{mean}, R_S	–	$ET_0 = \frac{\alpha}{\lambda}\frac{\Delta}{\Delta+\gamma}(R_n - G)$
Makkink	MK	$T_{\max}$, $T_{\min}$, T_{mean}, R_S	–	$ET_0 = 0.61\frac{\Delta}{\Delta+\gamma}\frac{R_S}{\lambda} - 0.12$
Turc	TU	T_{mean}, $T_{\max}$, $T_{\min}$, R_S, R_H	–	$ET_0 = a_T 0.013\frac{T_{mean}}{T_{mean}+15}\frac{23.8856R_S + 50}{\lambda}$ $R_H \geqslant 50 \rightarrow a_T = 1$ $R_H < 50 \rightarrow a_T = 1 + \frac{50 - R_H}{70}$
ET_o equations applied with limited data (second scenario)				
Penman-FAO-Monteith	PMFR_S est	T_{mean}, S_W, R_H	R_S	$R_S = 0.19.\ R_a\sqrt{T_{\max} - T_{\min}}$
Penman-FAO-Monteith	PMFS_W est	T_{mean}, R_S, R_H	S_W	Using exogenous SW values
Penman-FAO-Monteith	PMFR_S and S_W est	T_{mean}, R_H	R_S, S_W	As for the previous cases
Kimberly-Penman	KP R_S est	T_{mean}, S_W, R_H	R_S	As for the previous cases
Kimberly-Penman	KPS_W est	T_{mean}, R_S, R_H	S_W	As for the previous cases
Kimberly-Penman	KPR_S, S_W est	T_{mean}, R_S, R_H	R_S, S_W	As for the previous cases
Priestly-Taylor	PT R_S est	$T_{\max}$, $T_{\min}$, T_{mean}	R_S	As for the previous cases
Makkink	MK R_S est	$T_{\max}$, $T_{\min}$, T_{mean}	R_S	As for the previous cases
Turc	TU R_S est	T_{mean}, $T_{\max}$, $T_{\min}$, R_H	R_S	As for the previous cases
Turc	TU R_H est	T_{mean}, $T_{\max}$, $T_{\min}$, R_S	R_H	$R_H = e_a/e_s$
Turc	TU R_S and R_H est	T_{mean}, $T_{\max}$, $T_{\min}$	R_S, R_H	As for the previous cases

ET_o = reference [grass] evapotranspiration (mm day^{-1}), Δ = slope of the saturation vapor pressure function (kPa °C^{-1}), γ = psychometric constant (kPa °C^{-1}), R_n = net radiation (MJ m^{-2} day^{-1}),
G = Soil heat flux density (MJ m^{-2} day^{-1}), T_{mean} = mean air temperature (°C), S_W = average 24 h wind speed at 2 m height (m s^{-1}), es = saturation vapor pressure (kPa), ea = actual vapor pressure,
α = 1.26, λ = latent heat of the evaporation (MJ kg^{-1}), Ra = extraterrestrial radiation (mm day^{-1}), R_S = daily solar radiation (MJ m^{-2} day^{-1}), R_H = relative humidity (%), T_{max} = maximum air temperature (°C) and
T_{min} = minimum air temperature (°C). W_f is wind function that depends on wind speed and day number. "est" suffix represents the models fed with estimated variables.

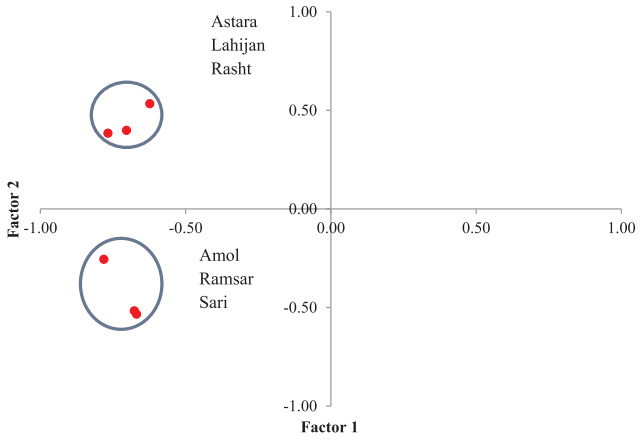

Fig. 1. Factors 1 and 2 of the PCA diagram of wind speed variable at the studied stations (explaining 87% of variance).

$$PE_*(forest) \leqslant \bar{\rho}.\ PE_*(tree) \quad (5)$$

Here, $\bar{\rho}.$ denotes the weighted correlation between the Y-h(X,Θ) and Y-h(X,Θ′) (Breiman, 2001).

Several numbers of trees were assessed in order to select the optimal random forest method at each case. Accordingly, the best cycle number was set as 15, on the basis of a trial and error process. Further, the percentage decrease of training error was 5%, minimum child node size was 5, and the maximum number of levels was 10 as advised by literature and assessed iteratively (Shiri, 2018).

2.4. Study flowchart

2.4.1. Scenarios adopted

In the present paper, the applied equations were implemented and assessed under full and limited data availability scenarios. In the first scenario, the models were applied using measured meteorological data as inputs (recorded time series of the meteorological variables). On the other hand, in the second scenario, the models were applied using estimated meteorological parameters as inputs. So, solar radiation, relative humidity and wind speed were assumed as missing variables and their values were estimated utilizing the approaches presented in Table 2. So, the lower side of Table 2 presents different alternatives adopted for estimating the missing variables. The estimation procedures of the variables were conducted according to FAO guidelines (Allen et al., 1998) for solar radiation and relative humidity. For the wind speed, average values of the other similar stations were used. In order to select the most similar stations to feed the wind speed values, a multiple sites over time (s-mode) principal component analysis (PCA) was applied. Among other alternatives (covariance; correlation), a correlation matrix was considered in this technique, since it can eliminate the differences in measurement units between the meteorological variables (Xystrakis and Matzarakis, 2011). Further, by this method, the locations with the same seasonal patterns of meteorological variables can be correlated together (Comrie and Glenn, 1998). Fig. 1 displays the projection of the stations on the factor plane. Accordingly, "Amol, Ramsar, Sari"; and "Astara, Lahijan, Rash" formed two separate clusters based on wind speed clustering procedure. Therefore the wind speed values of individual stations per each cluster were estimated by assuming the remaining two stations as ancillary sites. The estimation procedure was conducted using the average wind speed values of two

Table3
Adopted input configurations in concordance to the applied equations.

Model	T_{min}	T_{max}	T_{mean}	R_a	R_S	R_H	S_W
Temperature/humidity-based models							
RF1	■	■	■	■			
RF2	■	■	■	■		■	
HR	■	■	■	■			
PT R_S est	■	■	■	■			
TU R_S est	■	■	■	■		■	
TU R_S and R_H est	■	■	■	■			
MK R_S est	■	■	■	■			
Radiation-based models							
RF 3	■	■	■	■	■		
RF 4	■	■	■	■	■	■	
PT	■	■	■	■	■		
MK	■	■	■	■	■		
TU	■	■	■	■	■	■	
TU$R_H$est	■	■	■	■	■		
Combination-based models							
RF 5	■	■	■	■			■
RF 6	■	■	■	■		■	■
RF 7	■	■	■	■	■		■
RF 8	■	■	■	■	■	■	■
PFM R_S est	■	■	■	■		■	■
KP R_S est	■	■	■	■		■	■
PFM	■	■	■	■	■	■	■
PFM R_S and S_W est	■	■	■	■		■	
PFM S_W est	■	■	■	■	■	■	
KP S_W est	■	■	■	■	■	■	
KP	■	■	■	■	■	■	■
KP R_S, S_W est	■	■	■	■		■	

Note: the suffix "est" refers to the second scenario, where the models were established with one or more estimated meteorological variable(s).

ancillary stations per cluster.

2.4.2. Model implementation

All the applied equations were calibrated (using Eq. (1)) by considering the patterns of the first 5 years (50% of total patterns) as calibration patterns. The remaining patterns were then divided into two blocks (25%–25%) and used for testing and validating the revised equations, ensuring an independent test of the calibrated models. Attending to the RF models, several input configurations were built relying in the inputs of the applied equations. Table 3 summarized the applied input configurations by the RF models. Similarly to the empirical equations, the available data were divided into three blocks (50%–25%–25%) and the RF models were trained, tested and validated accordingly. An important shortcoming by the adopted scenarios would be the limitation of local assessment, but as mentioned, the goal was to assess the effect of using calculated input variables on ET_o equations performance. Further, due to the high number of approaches considered, a hold-out validation was used because k-fold validation would have involved unaffordable computational costs. It must be noted that the RF models were calibrated/trained using measured inputs.

2.5. Performance evaluation criteria

The assessment of the models was carried out using the scatter index (*SI*), the Nash-Sutcliffe coefficient (*NS*), the mean bias error (*MBE*) and the mean absolute error (*MAE*), expressions for which are as follows:

$$SI = \frac{RMSE}{PF\bar{M}ET_o} = \frac{\sqrt{\frac{1}{N}\sum_{i=1}^{N}(ET_{iM} - PFMET_{io})^2}}{PF\bar{M}ET_o} \quad (6)$$

$$MAE = \frac{\sum_{i=1}^{N}|PFMET_{io} - ET_{iM}|}{N} \quad (7)$$

$$NS = 1 - \frac{\sum_{i=1}^{N}(PFMET_{io} - ET_{iM})^2}{\sum_{i=1}^{N}(PFMET_{io} - PF\bar{M}ET_o)^2} \quad (8)$$

$$MBE = \frac{\sum_{i=1}^{N} ET_{iM} - PFMET_{io}}{N} \quad (9)$$

In these equations, ET_{iM} and $PFMET_{io}$ stand for the simulated and reference values at the *i*th time step, respectively. $E\bar{T}_M$ and $PF\bar{M}ET_o$ show the corresponding mean *ET* values, respectively. *N* is the number of available patterns for any specified (testing or validation) period.

An additional dimensionless indicator, namely, the relative *MAE* index was adopted for assessing the degree of the effectiveness of the calibration process in improving the equations' performances

$$r - MAE = 1 - \frac{MAE_{calibrated\ model}}{MAE_{noncalibrated\ model}} \quad (10)$$

3. Results and discussions

3.1. Alfalfa and grass ET ratio

The ratio of ET_r (calculated by KP equation variants) to ET_o (calculated by PFM) is usually applied to correct the ET_r values. Fig. 2 displays the K_r values for different KP versions (fed with original and estimated meteorological parameters) in the studied locations. Analyzing the values presented in this figure showed that K_r varied between 1.020 in Ramsar (for KP with R_S and KP with R_S and S_W estimated values) and 1.172 in Sari (for KP with R_S and S_W as estimated variables). Based on the average daily ET_o values presented in Table 1, differences between ET_r and ET_o in these stations are, respectively, 0.05 mm/day and 0.49 mm/day that are relatively small magnitudes. The mean K_r among all stations for all KP versions was 1.076. This value cannot correspond to the previous researches on KP applications under other climatic contexts. Analyzing KP for hyper-arid conditions, Shiri (2017) found an average K_r of 1.158 that was close to the suggested K_r value (=1.15) by e.g. Doorenbos and Pruitt (1977) and Jensen et al. (1990). Allen et al. (1994), on the other hand, reported mean K_r values between 1.12 and 1.39 for humid locations. While Irmak et al. (2003) adopted K_r = 1.18 for humid region of Florida, a minimum value of 1.03 for calm humid regions has been suggested in literature (e.g. Jensen et al., 1990) that is comparable value to those obtained in the present study. This partial review shows that differences between alfalfa and grass *ET* values in the studied sites have small magnitudes that might be linked to the lower wind speed and vapor pressure deficit values in these regions. Daily K_r values calculated with the original KP equation (KP using original meteorological variables) averaged over the months during the studied years have been shown in Fig. 1. According to this figure, the K_r values were lower than unity for cold season in all the studied stations, while it takes larger values during the warm period (maximum K_r was 1.179 in Sari for June).When the estimated R_S values were applied by KP equation, K_r variations and magnitudes were different (not presented here), so that it showed values over 1 during the year. In case of using estimated wind speed values, however, K_r variations and magnitudes were similar to the KP equation with original variables. Similar seasonal variations of K_r have been reported by Irmak et al (2003), too. This considerable seasonal variation of ET_r/ET_o relations during a year might be linked to the response of the target surfaces (grass and alfalfa) against the evaporative consumption, as discussed by Wright (1996).

3.2. Application of empirical equations

Table 4 sums up the local and global statistical indicators of the applied equations during the calibration procedure (2008–2012). Attending to the mean performance of the studied locations (global

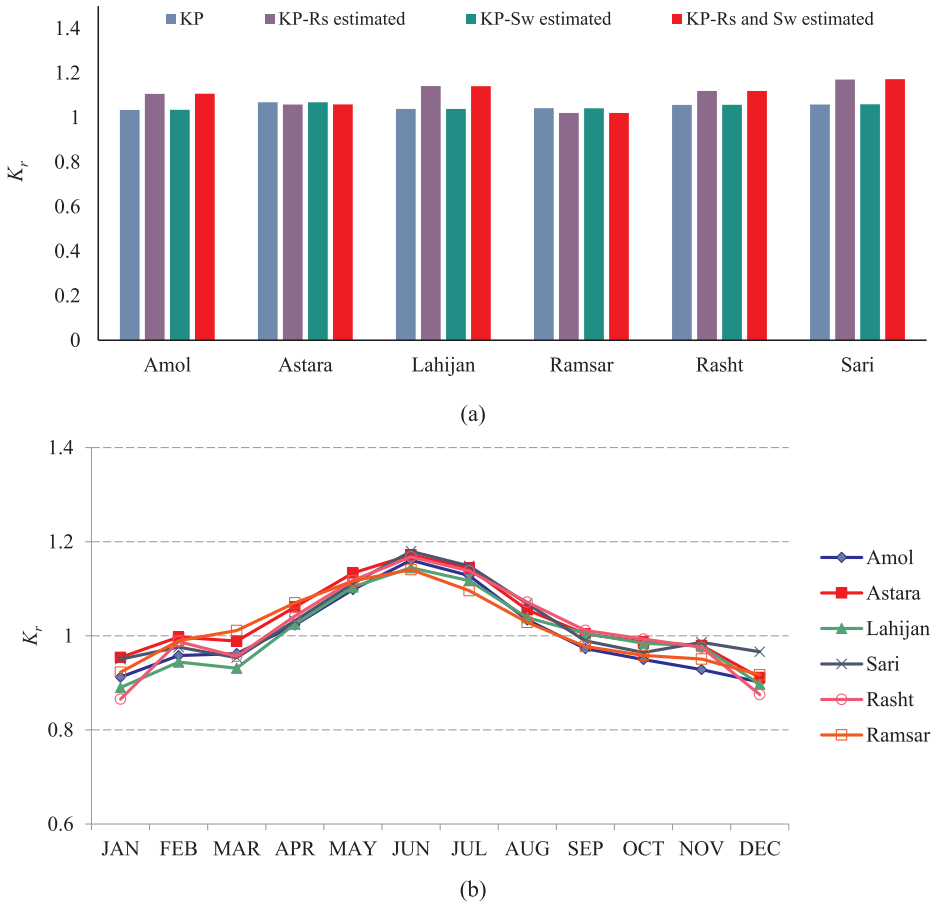

Fig. 2. a) *Kr* values of different Kimberly-Penman equation variants; b) Monthly *Kr* values of original KP equation.

indicators), the radiation-based PT equation outperformed the rest of the equations with the lowest *SI* (0.219) and *MAE* (0.449 mm/day) values, while the radiation-based TU equation provided the less accurate ET_o estimates with the highest *SI* (0.655) and *MAE* (1.598 mm/day). This confirms the results reported by Gunston and Batchelor (1983) for the regions with low wind speed values and Xiaoying and Erda (2005) for rainy locations/seasons. Analysis of the correlation values between the utilized meteorological variables and the equations' errors (Table 5) shows that the correlation between ET_o (calculated by PFM) and wind speed is very low (-0.051) when compared to the other parameters. This can explain the higher performance of the PT equation, in which the effect of wind speed (aerodynamic component) has been omitted and replaced by a constant value. The correlation between the models' error and wind speed is negligible, which could justify the more accurate performance of the radiation-based equations.

Regarding the equations applied with estimated (calculated) meteorological parameters, the PFM equation with estimated wind speed values (PFM S_W est; Table 4) provided the lowest *SI* values followed by the PT equation with estimated R_S values (PT R_S est; Table 4). This shows that the errors corresponding to S_W estimation were relatively smaller than those of R_S estimation. This might also might show a more relevant effect of solar radiation on ET_o than of wind speed, confirming the results obtained by Landeras et al. (2008) and Kwon and Choi (2011). On the other hand, Shiri (2017) confirmed a higher influence of wind speed on ET_o values in hyper-arid regions. A possible reason of this different behavior might be the wind speed characteristics in the studied locations as well as the stations' elevation. From Table 1, wind speed records showed similar average and standard deviation values between stations, so using wind speed values from ancillary stations (as estimated S_W values) would not involve large errors in ET_o computing procedure by the combination-based equations. Further, the temperature ranges are severely affected by air movement in the coast-sea interfaces at coastal regions which might be translated into less accurate R_S estimations from temperature range (Allen et al., 1998; Hargreaves and Allen, 2003). On the other hand, the studied regions have higher degrees of cloudiness during the year that can affect the performance of R_S estimation methods.

Overall, a preliminary ranking among the applied equations of both groups would lead to the following methods as the most accurate ones: combination-based PFM (with S_W est), PT, PT (with R_S est), MK, KP (with S_W est), HR and PFM (with R_S est). The Turc (TU) model and its variants couldn't outperform the other equations although it has been developed for humid locations. This might be due to the wind speed effect in the studied region. Trajkovic and Stojnic (2007) argued that the wind speed values lower than 1.5 m/s adversely affect the TU equation performance in humid location. Based on the wind speed values presented in Table 1, all stations have annual average wind speed values lower than this threshold that can explain the weak performance of this equation.

The analysis per station of the equations performance showed that the PFM equation with estimated wind speed values provided the lowest errors in comparison to other equations in all the locations, except at Amol and Sari, which present the lowest aridity index values. In these sites, the PT equation with estimated R_S values provided the most accurate estimates. Similar to the global assessment of the equations, the TU equation (and its variants) provided the worst ET_o estimates in all the locations.

A summary of the calibration constants of these equations has been listed in Table 4. Analyzing the calibration summary and *MBE* values, some remarks can be made. First, the temperature-based HR model overestimated ET_o values in all locations (with positive *MBE* values), which is in agreement with previously published literature (e.g.

Table 4
Summary of the models performance during the calibration period (2008–2012).

	Amol		Astara		Lahijan		Ramsar		Rasht		Sari		Global	
	SI	*MBE*	*SI*	*MBE*	*SI*	*MBE*	*SI*	*MBE*	*SI*	*MBE*	*SI*	*MBE*	*SI*	*MBE*
HR	0.220	0.345	0.214	0.085	0.298	0.452	0.211	0.017	0.277	0.385	0.250	0.519	0.245	0.333
PT	0.193	0.307	0.214	0.319	0.262	0.313	0.214	0.347	0.263	0.360	0.168	0.291	0.219	0.341
TU	0.642	−1.636	0.671	−1.619	0.689	−1.596	0.640	−1.533	0.670	−1.556	0.676	−1.648	0.665	−1.141
MK	0.194	−0.357	0.221	−0.331	0.265	−0.334	0.197	−0.332	0.240	−0.327	0.228	−0.372	0.224	−0.232
KP	0.143	0.104	0.169	0.164	0.203	0.111	0.146	0.119	0.209	0.167	0.176	0.172	0.437	0.214
PT *Rs* est	0.427	0.584	0.351	0.352	0.518	0.640	0.344	0.289	0.512	0.645	0.470	0.698	0.174	0.500
MK *Rs* est	0.285	−0.059	0.357	−0.270	0.350	−0.025	0.412	−0.369	0.346	−0.002	0.298	−0.073	0.341	−0.116
PFM*Rs* est	0.237	0.193	0.218	0.025	0.267	0.233	0.248	−0.042	0.263	0.204	0.257	0.287	0.248	0.178
PFM*Sw* est	0.158	0.155	0.113	0.012	0.150	−0.025	0.117	−0.025	0.128	0.039	0.252	0.339	0.153	0.096
PFM*Rs* and *Sw* est	0.312	0.338	0.255	0.034	0.301	0.207	0.279	−0.068	0.297	0.239	0.400	0.600	0.307	0.256
KP *Rs* est	0.335	0.324	0.306	0.191	0.411	0.370	0.288	0.073	0.399	0.393	0.390	0.495	0.355	0.334
KP *Sw* est	0.205	0.106	0.228	0.164	0.274	0.110	0.200	0.119	0.278	0.167	0.234	0.176	0.237	0.162
KP *Rs* and *Sw* est	0.336	0.326	0.306	0.191	0.411	0.370	0.288	0.073	0.399	0.394	0.391	0.499	0.355	0.335
TU *Rs* est	0.877	−1.513	0.971	−1.595	0.893	−1.446	0.975	−1.550	0.908	−1.424	0.878	−1.467	0.917	−1.071
TU R_H est	0.920	−1.634	0.954	−1.614	0.951	−1.591	0.931	−1.532	0.946	−1.552	0.933	−1.640	0.939	−1.138
TU *Rs* and R_H est	0.876	−1.511	0.967	−1.589	0.888	−1.439	0.974	−1.548	0.904	−1.417	0.937	−1.648	0.924	−1.089

Calibration summary (*a* and *b* are regression coefficients of calibration equation; See equation1)

	a	*b*	*a*	*b*	*A*	*b*	*A*	*b*	*a*	*b*	*a*	*b*
HR	0.898	−0.022	0.997	−0.076	0.855	0.019	1.091	−0.226	0.921	−0.142	0.951	−0.352
PT	0.833	0.216	0.878	0.060	0.870	0.091	0.850	0.106	0.835	0.145	0.862	0.145
TU	2.336	0.042	2.280	0.123	2.347	−0.017	2.360	−0.027	2.293	0.066	2.356	0.000
MK	1.130	0.036	1.116	0.047	1.135	0.002	1.114	0.064	1.099	0.092	1.110	0.097
KP	0.847	0.346	0.854	0.268	0.877	0.246	0.870	0.245	0.839	0.296	0.835	0.329
PT *Rs* est	0.782	0.162	0.909	−0.064	0.787	0.092	0.939	−0.108	0.808	−0.001	0.829	−0.089
MK *Rs* est	1.095	−0.204	1.198	−0.223	1.034	−0.121	1.320	−0.369	1.107	−0.290	1.172	−0.579
PFM*Rs* est	0.924	0.038	1.006	−0.038	0.908	0.045	1.053	−0.097	0.957	−0.077	0.967	−0.184
PFM*Sw* est	0.928	0.059	0.990	0.016	1.019	−0.027	1.009	0.001	0.963	0.063	0.874	0.063
PFM*Rs* and *Sw* est	0.858	0.111	0.988	0.003	0.917	0.044	1.064	−0.098	0.923	−0.015	0.855	−0.097
KP *Rs* est	0.796	0.319	0.862	0.225	0.802	0.258	0.924	0.137	0.818	0.174	0.813	0.133
KP *Sw* est	0.846	0.347	0.854	0.268	0.877	0.247	0.870	0.245	0.839	0.298	0.834	0.328
KP *Rs* and *Sw* est	0.796	0.320	0.862	0.225	0.802	0.259	0.924	0.137	0.817	0.175	0.812	0.133
TU *Rs* est	2.205	−0.071	2.359	−0.016	2.106	−0.042	2.661	−0.323	2.229	−0.151	2.362	−0.433
TU R_H est	2.335	0.038	2.267	0.128	2.342	−0.023	2.362	−0.032	2.291	0.058	2.337	0.006
TU *Rs* and R_H est	2.196	−0.064	2.333	0.001	2.073	−0.012	2.643	−0.308	2.195	−0.121	2.356	0.000

Table 5
Correlation matrix of the used meteorological variables and models' errors.

	T_{min}	T_{max}	T_{mean}	R_H	S_W	R_S	ET_o-PFM
T_{min}	1.000	0.867	0.952	−0.022	−0.059	0.492	0.741
T_{max}	0.867	1.000	0.963	−0.020	−0.149	0.703	0.879
T_{mean}	0.952	0.963	1.000	−0.045	−0.090	0.645	0.855
R_H	−0.022	−0.020	−0.045	1.000	−0.955	−0.175	−0.136
S_W	−0.059	−0.149	−0.090	−0.955	1.000	0.006	−0.051
R_S	0.492	0.703	0.645	−0.175	0.006	1.000	0.901
ET_o -PFM	0.741	0.879	0.855	−0.136	−0.051	0.901	1.000
ET_o-HR	0.224	0.250	0.230	−0.004	−0.046	0.075	0.197
ET_o-PT	0.163	0.220	0.202	−0.108	0.024	0.188	0.329
ET_o-TU	0.650	0.776	0.752	−0.128	−0.058	0.776	0.939
ET_o-MK	0.211	0.267	0.240	−0.050	−0.054	0.073	0.319
ET_o-KP	0.125	0.202	0.171	−0.106	−0.001	0.128	0.294
RF1	0.268	0.242	0.249	−0.028	−0.018	0.082	0.209
RF2	0.271	0.262	0.267	−0.051	−0.001	0.154	0.254
RF3	0.032	0.060	0.045	−0.035	−0.021	−0.010	0.111
RF4	0.042	0.069	0.053	−0.038	−0.016	0.002	0.119
RF5	0.270	0.268	0.264	−0.039	−0.018	0.088	0.243
RF6	0.242	0.220	0.232	−0.028	−0.008	0.092	0.194
RF7	0.031	0.034	0.026	−0.027	−0.011	−0.009	0.071
RF8	0.046	0.074	0.060	−0.037	−0.018	0.002	0.126

Droogers and Allen, 2002; Xu and Singh, 2002). The overestimation of HR equation in these locations might be due to either higher temperature ranges (Gavilan et al., 2006) or lower wind speed values (Allen et al., 1998) as can be seen in Table 1. Next, the radiation-based PT equation overestimated ET_o records in all the locations, confirming the results of e.g. Benli et al. (2010), Berengena and Gavilàn (2005), and Yoder et al. (2005). Similar trend can be seen for PT equation fed with estimated R_S values. Using the calibration procedure, the original advectivity constant of PT equation ($\alpha = 1.26$) was revised in all the stations as follows: 1.05, 1.10, 1.09, 1.07, 1.05, and 1.086 for Amol, Astara, Lahijan, Ramsar, Rasht and Sari, respectively. These values are not in agreement neither with the suggested bound of advectivity

constant range by Viswanadham et al. (1991) [1.2 < α < 1.3] nor with Pereira (2004) who proposed α = 1.27 for grass cover in humid tropical regions. However, Eaton et al. (2001) found α values between 1.07 and 1.10 for wetlands that are comparable regions to the studied costal sites. Sentelhas et al. (2010) also reported α < 1.26 values (overestimation trend) for the cold climates of Canada. Suleiman and Hoogenboom (2007), on the other hand, argued that PT equation has seasonal variations and shows overestimation trend for the warm season in coastal and mountain regions, while it underestimated the ET_o values for the cold season. Overall, the values of α depend on the specified climatic conditions, under which the study has been conducted, and the revised coefficients in the present study (after adjustment/calibration) are in agreement with literature for coastal humid regions.

The MK and TU equations variants, however, underestimated ET_o values in all sites (see Table 4). Shiri et al. (2014) argued that MK usually gives underestimated simulations of ET_o for different climatic contexts. They also found that in the regions with lower wind speed values, TU equations tend to underestimate ET_o. This is in agreement with the statements presented in this research. This shows that the original constant values of MK and TU equations (0.61 and 0.13 a_T, respectively) are low and they should take higher values for improving the ET_o simulations in the studied humid locations. The original constant value of the MK equation can provide reasonable ET_o estimates in humid locations (Xu and Chen, 2005; Cristea et al., 2013), which does not fit with the findings of the present paper. Finally, among the combination-based equations, KP variants overestimated ET_o values in all locations. However, PFM variants provided both over/underestimated ET_o values in the stations and no general conclusions could be obtained for their trends. The overestimation trend of the PFM equation relying on estimated R_S values has been observed for humid locations in the literature (e.g. Fisher and Pringle, 2013; Todorovic et al., 2013). Nonetheless, overestimation of ET_o using the PFM equation with estimated solar radiation and wind speed has been also previously encountered (Gelcer et al., 2010).

3.3. Calibration of ET_o equations

Fig. 3 displays the *r-MAE* values of the calibrated equations during the validation period for the studied stations. In all locations, the lowest *r-MAE* values correspond to the TU equation, which shows the lower impact of the calibration process for increasing the performance accuracy of this equation. The highest *r-MAE* values (the highest impact of calibration on improving the equations' performances) are observed for combination-based models, except in Sari and Amol, where PT and MK equations gave the maximum values for this indicator. The higher values of this indicator in the mentioned cases show the significant impact of the calibration process on the performance accuracy of these equations. However, this indicator just shows the degree of the effectiveness of the calibration procedure, so it can't be applied for assessing the performance accuracy of the calibrated equations. In Fig. 4, the global *SI* values of the equations during the testing and validation periods have been presented. The figure clearly shows that the performance accuracies of the calibrated PFM variants are higher than the rest of the applied equations in both the testing and validation periods, confirming the conclusions reported by Shiri (2017) for hyper-arid regions. Meanwhile, calibrated PFM equation that used estimated wind speed values (CPFM S_W est) surpassed the other variants with the lowest global *SI* values: 0.085 and 0.081 for testing and validation periods, respectively.

3.4. Random forest (RF) models

Figs. 5 and 6 show the global and local *SI* values of the applied RF models during the testing and validation periods (see Table 3 for input configurations). The global values correspond to the mean performance of the models in all stations. In both the periods, the global *SI* values are low, indicating the promising performance of all the applied RF models. As could be anticipated, combination-based RF8 model comprising all the available meteorological variables outperformed the other models in the testing and validation periods, followed by the radiation-based RF4 model that included the air temperature, solar radiation and humidity variables. Comparing the radiation- and combination-based models, it might be stated that the inclusion of solar radiation is more important than of relative humidity and wind speed variables. This might show again a higher significance of R_S on ET_o. Correlation analysis presented in Table 5 confirms this statement, too. Nevertheless, the temperature-based RF1 model was less accurate than the rest of the models, although its *SI* values were quite low (0.056 for both the periods). The assessment per station of the models showed that the RF models provided the highest *SI* values in Rasht and Ramsar, which can be due to the slightly higher values of skewness coefficient for ET_o records (values not shown) in these locations. However, the magnitudes of relative errors (*SI*) are lower than 0.1 in all the locations. Hence, it might be stated that all the applied RF models could be successfully applied in simulating ET_o values in the studied coastal humid regions.

3.5. RF vs. Classical methods

The global ranking of the applied RF models and calibrated equations based on the validation period's (2016–2017) indicators has been summarized in Table 6. The reported values are the mean of the individual stations' indicators. The most and less accurate results in term of the presented indicators belonged to, respectively, RF8 and calibrated PT (CPT) equation. More specifically, among the temperature-based models, RF2 (comprising temperature, extraterrestrial radiation and relative humidity inputs) surpassed the other models, followed by RF1 (comprising temperature, extraterrestrial radiation inputs), calibrated HR (CHR), CTU R_S and R_H est, CTU R_S est, CPT R_S est, and CMK R_S est (see Table 2 for abbreviations). Attending to the radiation-based models, RF4 and RF3 provided similar results and outperformed the calibrated empirical equations. Here, as can be seen in Table 6, the calibrated Turc model (CTU R_H est) surpassed CTU (using measured meteorological data), CMK and CPT equations, which is not in agreement with the outcomes of Landeras et al. (2008) and Shiri (2017) for the humid and hyper-arid regions, respectively. Regarding the combination-based models, RF8 provided the most accurate results followed by the CPFM S_W est and RF7 models. This is an interesting outcome, because the calibrated PFM model with estimated wind speed values showed higher accuracy than the RF7 model (that comprises all necessary variables except R_H). Again, the obtained results might question the suitability of the combination-based machine learning models under different climatic conditions (e.g. Shiri et al., 2012). This might show the significant effect of relative humidity, which is a very important factor in coastal regions, although it presented minor negative correlation (mean value of −0.136 for the studied region) with ET_o. Moreover, the wind speed estimation technique adopted in the present study produced reliable wind speed data and, subsequently, ET_o estimations. An overall analysis of the correlation matrix (Table 5) revealed that air temperature showed considerable positive correlations with models' errors (both equations and RF models), while wind speed and relative humidity always presented negative small correlation values. Solar radiation shows positive correlations, except with RF3 and RF7 models. However, its correlation magnitudes with models' errors are lower than those of air temperature. In spite of that, considering the correlations between ET_o and meteorological variables, solar radiation presented the highest correlation values that may reflect the higher importance of R_S on ET_o. This can be evaluated simply by taking into consideration the combination-based KP equation, in which the energy and aerodynamic components can be quantified separately. The ratio between the aerodynamic and energy components in this equation for Amol, Astara, Lahijan, Ramsar, Rasht and Sari, were respectively,

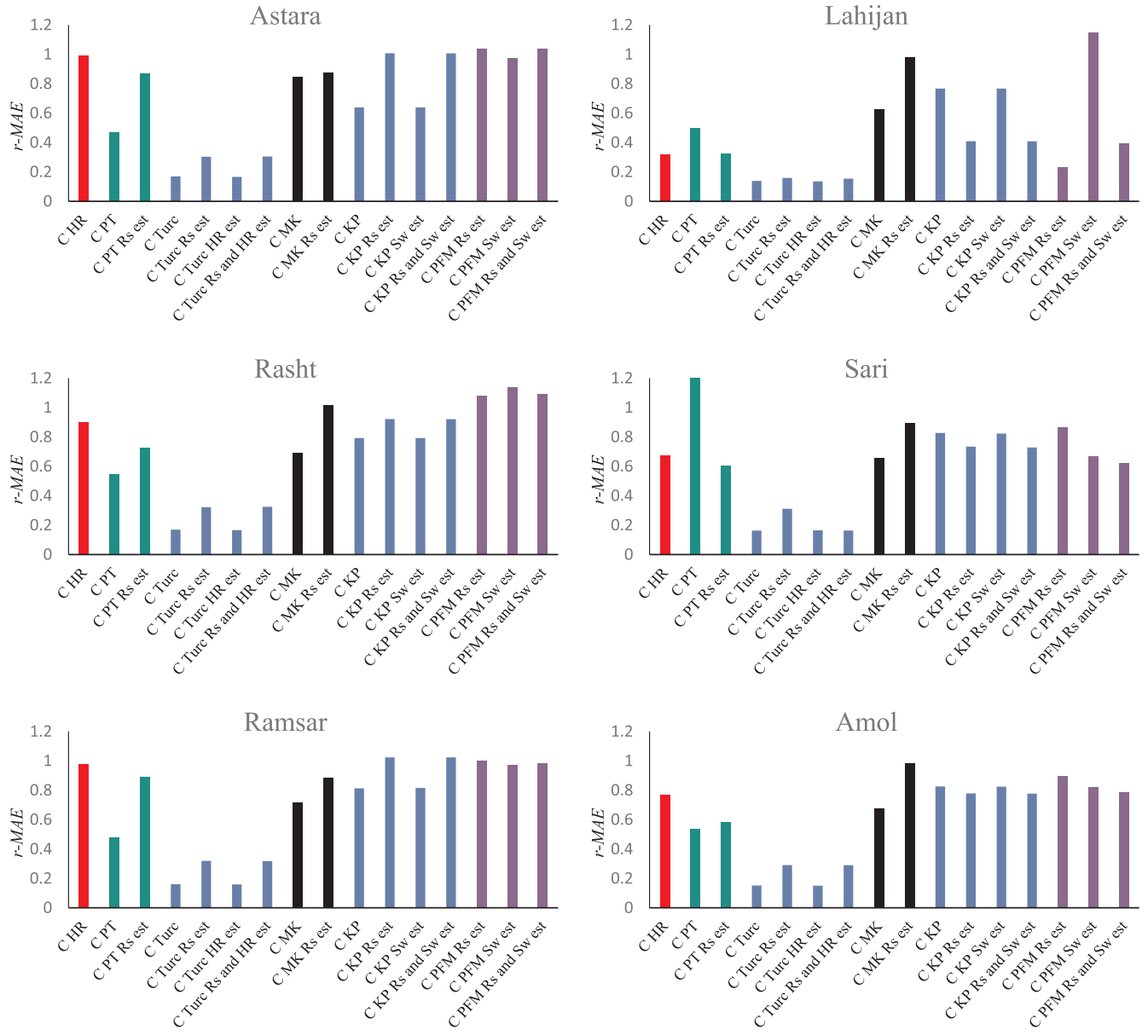

Fig. 3. *r-MAE* (relative mean squared error) values of the calibrated equations during the validation period for each station.

0.164, 0.104, 0.091, 0.091, 0.094, and 0.124. These values clearly show the negligible impact of wind speed in the final ET_o magnitudes in the studied regions and confirms the statements extracted from the correlation analysis.

Summarizing, the present paper aimed at assessing the missing values supplanting on various empirical equations and comparing the results with random forest (RF) models in humid regions. Extending the boundaries of this study might be carried out through evaluation of the calibrated empirical equations on monthly basis to check the seasonality effect, accurately. Further, the impact of relative humidity was monotonously fluctuating among the stations and adopted scenarios, which might be subject for future studies. Further detailed studies should be also performed for more detailed assessment of the classical TURC model that has been developed for humid regions, while provided the less accurate results among others. Finally, considering a larger number of stations for the most promising approaches, as well as verifying the results with experimental *ET* values along with repeating the procedures after a preliminary clustering analysis might be approaches for future studies to strengthen the statements of the present study.

4. Conclusions

This study assessed the effect of supplanting missing measured meteorological variables with calculated values for estimating reference evapotranspiration with classical and random forest approaches at coastal humid regions. Based on the obtained results, some concluding remarks were highlighted as follows:

1. Analyzing the global indicators, it is clear that the radiation-based PT equation outperformed the rest of the equations, while the radiation-based TU equation provided the less accurate ET_o estimations.
2. Temperature-based Hargreaves-Samani, radiation-based Priestley-Taylor and combination-based Kimberly-Penman variants overestimated the ET_o values in all locations.
3. MK and TU equations underestimated ET_o in all locations.
4. PFM variants showed both over/underestimated patterns in the stations
5. The effect of using estimated solar radiation values is more relevant than of using estimated wind speed and relative humidity values.

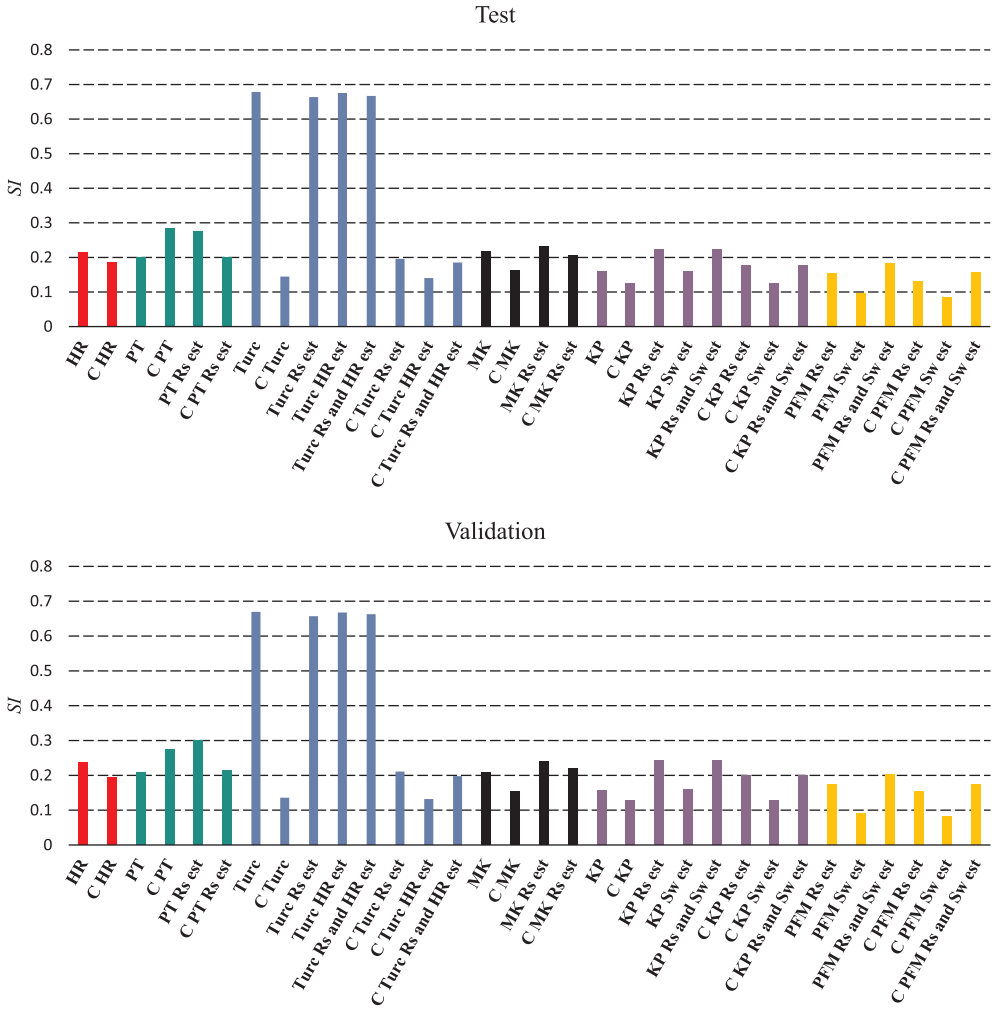

Fig. 4. Global (mean) *SI* values of the applied equations during the testing and validation periods.

6. Estimating solar radiation from temperature range involves higher errors in cloudy regions.
7. The ET_r/ET_o values were lower than unity for cold season in all the studied stations, while it takes larger values during the warm period.
8. When the estimated wind speed values were used by KP, K_r variations and magnitudes were similar to the KP equation with original variables.

CRediT authorship contribution statement

Sepideh Karimi: Conceptualization, Software, Investigation, Writing - original draft, Writing - review & editing. **Jalal Shiri:** Conceptualization, Methodology, Writing - original draft, Formal analysis. **Pau Marti:** Writing - original draft, Validation.

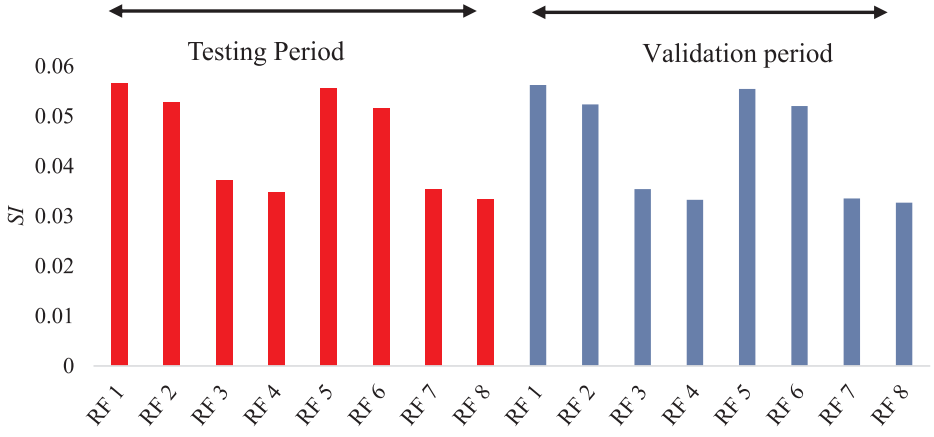

Fig. 5. Global *SI* values of the random forest models during the testing and validation periods.

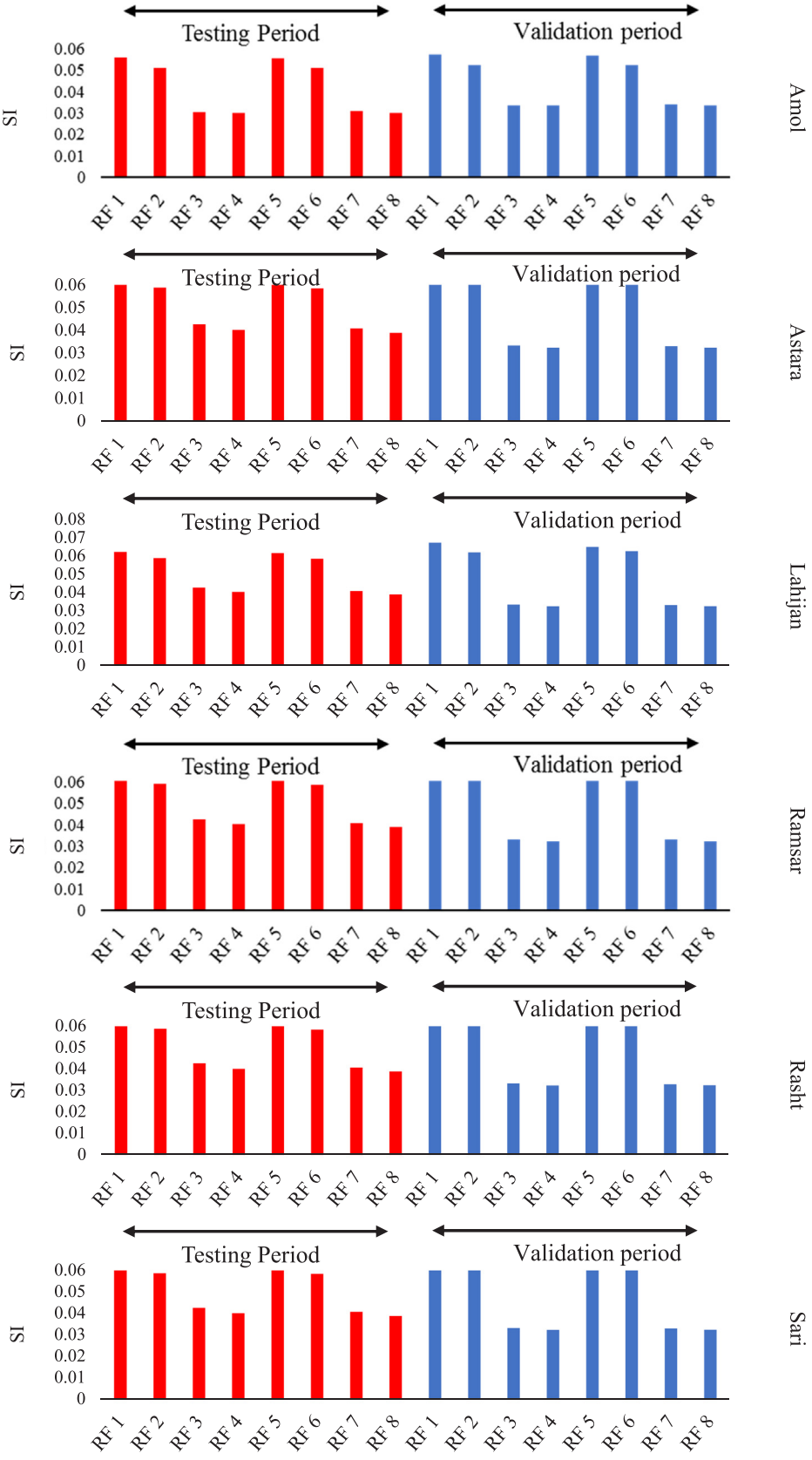

Fig. 6. *SI* values of the RF models at each station during the test and validation periods.

Table 6
Mean (global) rank of the applied models based on validation statistics.

Rank	Model	*SI*			*MAE* (mm day^{-1})			*NS*		
		Max	Mean	Min	MAX	Mean	Min	Max	Mean	Min
1	RF 8	0.039	0.033	0.027	0.199	0.186	0.166	0.985	0.966	0.967
2	C PFM S_w est	0.056	0.033	0.068	0.202	0.127	0.096	0.975	0.979	0.958
3	RF 7	0.041	0.033	0.028	0.214	0.191	0.174	0.972	0.964	0.952
4	RF 4	0.039	0.033	0.027	0.202	0.189	0.167	0.975	0.966	0.956
5	RF 3	0.044	0.035	0.031	0.221	0.199	0.18	0.969	0.962	0.944
6	C KP	0.074	0.060	0.044	0.245	0.216	0.193	0.965	0.948	0.913
7	C KP S_w est	0.074	0.065	0.045	0.246	0.217	0.193	0.965	0.948	0.913
8	RF 2	0.062	0.053	0.042	0.402	0.347	0.278	0.939	0.910	0.877
9	RF 6	0.063	0.053	0.043	0.409	0.350	0.285	0.938	0.910	0.874
10	RF 5	0.065	0.057	0.044	0.416	0.378	0.293	0.934	0.895	0.865
11	RF 1	0.067	0.057	0.042	0.430	0.376	0.276	0.938	0.895	0.866
12	C Turc R_H est	0.161	0.132	0.107	0.280	0.255	0.215	0.961	0.944	0.925
13	C Turc	0.167	0.136	0.111	0.280	0.259	0.222	0.957	0.941	0.920
14	C MK	0.190	0.154	0.115	0.342	0.300	0.232	0.955	0.924	0.896
15	C PFM R_S est	0.195	0.155	0.033	0.371	0.306	0.068	0.996	0.915	0.880
16	C PFM R_S and S_w est	0.213	0.174	0.072	0.411	0.343	0.128	0.982	0.898	0.857
17	C HR	0.241	0.193	0.097	0.468	0.396	0.182	0.968	0.877	0.833
18	C KP R_S est	0.250	0.198	0.121	0.438	0.384	0.222	0.950	0.873	0.821
19	C KP R_S and S_w est	0.250	0.198	0.121	0.437	0.384	0.221	0.950	0.872	0.820
20	C Turc R_S and R_H est	0.265	0.198	0.109	0.515	0.411	0.219	0.959	0.868	0.799
21	C Turc R_S est	0.264	0.211	0.114	0.513	0.444	0.226	0.956	0.854	0.800
22	C PT R_S est	0.274	0.213	0.143	0.480	0.415	0.275	0.930	0.854	0.785
23	C MK R_S est	0.284	0.220	0.118	0.557	0.461	0.238	0.952	0.841	0.768
24	C PT	0.929	0.275	0.122	2.318	0.587	0.222	0.952	0.504	−1.638

Declaration of Competing Interest

The authors declare that they have no known competing financial interests or personal relationships that could have appeared to influence the work reported in this paper.

Acknowledgement

The present study was partially supported by University of Tabriz (Vice-chancellory for Research and Technology).

References

Abdullah, S.S., Malek, A.M., Abdullah, N.S., Kisi, O., Yap, K.S., 2015. Extreme Learning Machines: a new approach for prediction of reference evapotranspiration. J. Hydrol. 527, 184–195.
Allen, R.G.L.S., Pereira, D., Raes, M., 1998. Smith Crop evapotranspiration. Guide lines for computing crop evapotranspiration. FAO Irrigation and Drainage, Paper no. 56. FAO, Rome.
Allen, R.G., Smith, M., Pereira, L.S., 1994. An update for the definition of reference evapotranspiration. ICID Bull. 43, 1–34.
Benli, B., Bruggeman, A., Oweis, T., Ustun, H., 2010. Performance of Penman-Monteith FAO56 in a semiarid highland environment. J. Irrig. Drain. Eng. 136 (11), 757–765.
Berengena, J., Gavilàn, P., 2005. Reference evapotranspiration estimation in a highly advective semiarid environment. J. Irrig. Drain. Eng. 131 (2), 147–163.
Bourletsikas, A., Argyrokastritis, I., Proutsos, N., 2018. Comparative evaluation of 24 reference evapotranspiration equations applied on an evergreen broad-leaved forest. Hydrol. Res. 49 (4), 1028–1041.
Breiman, L., 2001. Random forests. Mach. Learn. 45 (1), 5–32.
Chen, D., Gong, L., Xu, C.-Y., Halldin, S., 2007. A high-resolution, gridded dataset for monthly temperature normals (1971–2000) in Sweden. Geogr. Ann. Ser. A 89 (4), 249–261.
Comrie, A.C., Glenn, E.C., 1998. Principal components-based regionalization of precipitation regimes across the southwest United States and northern Mexico, with an application to monsoon precipitation variability. Clim. Res. 10 (3), 201–215.
Cordova, M., Carillo-Rioss, G., Crespo, P., Wilcox, B., Celleri, R., 2015. Evaluation of the Penman-Monteith (FAO 56 PM) method for calculating reference evapotranspiration using limited data. Mt. Res. Dev. 35 (3), 230–239.
Cristea, N.C., Kampf, S.K., Burges, S.J., 2013. Revised coefficients for Priestley-Taylor and Makkink-Hansen equations for estimating daily reference evapotranspiration. J. Hydrol. Eng. 18, 1289–1300.
Djaman, K., Irmak, S., Kabenge, I., Futakuchi, K., 2016. Evaluation of FAO-56 Penman-Monteith model with limited data and the Valiantzas models for estimating Grass-Reference evapotranspiration in Sahelian conditions. J. Irrig. Drain. Eng. 04016044, 1–14.
Doorenbos, J., Pruitt, W.O., 1977. Crop water requirements. FAO Irrigation and Drainage, Paper no. 24. FAO, Rome.
Droogers, P., Allen, R.G., 2002. Estimating reference evapotranspiration under inaccurate data conditions. Irrig. Drain. Syst. 16 (1), 33–45.
Eaton, A.K., Rouse, W.R., Lafleur, P.M., Marsh, P., Blanken, P.D., 2001. Surface energy balance of the western and central Canadian subarctic: variations in the energy balance among five major terrain types. J. Clim. 14 (17), 3692–3703.
Farzanpour, H., Shiri, J., Sadraddini, A.A., Trajkovic, S., 2019. Global comparison of 20 reference evapotranspiration equations in a semi-arid region of Iran. Hydrol. Res. 50 (1), 282–300.
Feng, Y., Cui, N., Zhao, L., Hu, X., Gong, D., 2016. Comparison of ELM, GANN, WNN and empirical models for estimating reference evapotranspiration in humid region of Southwest China. J. Hydrol. 536, 376–383.
Feng, Y., Cui, N., Gong, D., Zhang, Q., Zhao, L., 2017. Evaluation of random forests and generalized regression neural networks for daily reference evapotranspiration modeling. Agric. Water Manage. 193, 163–173.
Fisher, D., Pringle III, H., 2013. Evaluation of alternative methods for estimating reference evapotranspiration. Agric. Sci. 4, 51–60.
Gao, F., Feng, G., Ouyang, Y., Wang, H., Fisher, D., Adeli, A., Jenkins, J., 2017. Evaluation of reference evapotranspiration methods in arid, semiarid, and humid region. J. Am. Water. Res. Assoc. 53 (4), 791–808.
Gavilan, P., Lorite, I.J., Tornero, S., Berengena, J., 2006. Regional calibration of Hargreaves equation for estimating reference ET in a semiarid environment. Agirc. Water Manage. 81, 257–281.
Gelcer, E.M., Fraisse, C.W., Sentelhas, P.C., 2010. Evaluation of methodologies to estimate reference evapotranspiration in Florida. Proc. Fla. State Hort. Soc. 123, 189–195.
Gong, L., Xu, C.Y., Chen, D., Halldin, S., Chen, Y.D., 2006. Sensitivity of the Penman-Monteith reference evapotranspiration to key climatic variables in the Changjiang (Yangtze River) basin. J. Hydrol. 329, 620–629.
Guitjens, J.C., 1982. Models of Alfalfa yield and evapotranspiration. J. Irrig. Drain. Div. Proc. Am. Soc. Civ. Eng. 108 (IR3), 212–222.
Gunston, H., Batchelor, C.H., 1983. A comparison of the Priestley-Taylor and Penman methods for estimating reference crop evapotranspiration in tropical countries. Agirc. Water Manage. 6 (1), 65–77.
Harbeck Jr., G.E., 1962. A practical field technique for measuring reservoir evaporation utilizing mass-transfer theory. In: U.S Geol. Surv., Paper 272-E, pp. 101–105.
Hargreaves, G.H., Allen, R.G., 2003. History and evaluation of Hargreaves evapotranspiration equation. J. Irrig. Drain. Eng. 129 (1), 53–63.
Hargreaves, G.L., Samani, Z.A., 1982. Estimating potential evapotranspiration. J. Irrig. Drain. Eng. ASCE 108 (3), 225–230.
Hastie, T., Tibshirani, R., Friedman, J., 2009. The Elements of Statistical Learnin. Springer, New York.
Huang, G., Wu, L., Ma, X., Zhang, W., Fan, J., Yu, X., Zeng, W., Zhou, H., 2019. Evaluation of CatBoost method for prediction of reference evapotranspiration in humid regions. J. Hydrol. 574, 1029–1041.
Irmak, S., Allen, R.G., Whitty, E.B., 2003. Daily grass and alfalfa-reference evapotranspiration estimates and alfalfa-to-grass evapotranspiration ratios in Florida. J. Irrig. Drain. Eng. ASCE 129 (5), 360–370.
Jabloun, M., Sahli, A., 2008. Evaluation of FAO-56 methodology for estimating reference evapotranspiration using limited climatic data: application to Tunisia. Agric. Water

Manage. 95, 707–715.
Jensen, M.E., Burman, R.D., Allen, R.G., 1990. Evapotranspiration and irrigation water requirements. ASCE Manuals and Reports on Engineering Practices no. 70. American Society of Civil Engineers.
Karimi, S., Kisi, O., Kim, S., Nazemi, A.H., Shiri, J., 2017. Modeling daily reference evapotranspiration in humid locations of South Korea using local and cross-station data management scenarios. Int. J. Clim. 37 (3), 3238–3246.
Karimi, S., Shiri, J., Kisi, P., Xu, T., 2018. Forecasting daily streamflow values: assessing heuristic models. Hydrol. Res. 49 (3), 658–669.
Kwon, H., Choi, M., 2011. Error assessment of climate variables for FAO-56 reference evapotranspiration. Meteorol. Atmos. Phys. 112, 81–90.
Landeras, G., Ortiz-Barredo, A., Lopez, J.J., 2008. Comparison of artificial neural network models and empirical and semi-empirical equations for daily reference evapotranspiration estimation in the Basque Country (Northern Spain). Agirc. Water Manage. 95, 553–565.
Makkink, G.F., 1957. Testing the Penman formula by means of lysimeters. J. Inst. Water Eng. 11 (3), 277–288.
Pereira, A.R., 2004. The Priestley-Taylor parameter and the decoupling factor for estimating reference evapotranspiration. Agric. Forest. Meteorol. 125 (3–4), 305–313.
Popova, Z., Kercheva, M., Pereira, L.S., 2006. Validation of the FAO methodology for computing ETo with limited data: application to South Bulgaria. Irrig. Drain. 55, 201–215.
Priestley, C.H.B., Taylor, R.J., 1972. On the assessment of surface heat flux and evaporation using large-scale parameters. Mon. Weather Rev. 100 (2), 81–92.
Rojas, J.P., Sheffield, R.E., 2013. Evaluation of daily reference evapotranspiration methods as compared with the ASCE-EWRI Penman-Monteith equation using limited weather data in Northeast Louisiana. J. Irrig. Drain. Eng. 139 (4), 285–292.
Sentelhas, P.C., Gillespite, T.J., Santos, E.A., 2010. Evaluation of FAO Penman-Monteith and alternative methods for estimating reference evapotranspiration with missing data in Southern Ontario, Canada. Agirc. Water Manage. 97, 635–644.
Shiri, J., 2017. Evaluation of FAO56-PM, empirical, semi-empirical and gene expression programming approaches for estimating daily reference evapotranspiration in hyper-arid regions of Iran. Agric. Water Manage. 188, 101–114.
Shiri, J., 2018. Improving the performance of the mass transfer-based reference evapotranspiration estimation approaches through a coupled wavelet random forest methodology. J. Hydrol. 561, 737–750.
Shiri, J., Kisi, O., Landeras, G., Lopez, J.J., Nazemi, A.H., Stuyt, L.C.P.M., 2012. Daily reference evapotranspiration modeling by using genetic programming approach in the Basque Country (Northern Spain). J. Hydrol. 414–415, 302–316.
Shiri, J., Nazemi, A.H., Sadraddini, A.A., Landeras, G., Kisi, O., FakheriFard, A., Marti, P., 2014. Comparison of heuristic and empirical approaches for estimating reference evapotranspiration from limited inputs in Iran. Comput. Electron. Agric. 108, 230–241.
Stockle, C.O., Kjelgaard, J., Bellocchi, G., 2004. Evaluation of estimated weather data for calculating Penman-Monteith reference crop evapotranspiration. Irrig. Sci. 23, 39–46.
Suleiman, A.A., Hoogenboom, G., 2007. Comparison of Priestley-Taylor and FAO-56 Penman-Monteith for daily reference evapotranspiration estimation in Georgia, USA. J. Irrig. Drain. Eng. 133, 175–182.
Tabari, H., 2010. Evaluation of reference crop evapotranspiration equations in various climates. Water Res. Manage. 24, 2311–2337.
Tabari, H., Kisi, O., Ezani, A., Hosseinzadeh Talaee, P., 2012. SVM, ANFIS, regression and climate based models for reference evapotranspiration modeling using limited climatic data in a semi-arid highland environment. J. Hydrol. 444–445, 78–89.
Tabari, H., Grismer, M.A., Trajkovic, S., 2013. Comparative analysis of 31 reference evapotranspiration methods under humid conditions. Irrig. Sci. 31 (2), 107–117.
Todorovic, M., Karic, B., Pereira, L.S., 2013. Reference evapotranspiration estimate with limited weather data across a range of Mediterranean climates. J. Hydrol. 481, 166–176.
Torres, A.F., Walker, W.R., McKee, M., 2011. Forecasting daily potential evapotranspiration using machine learning and limited climatic data. Agirc. Water Manage. 98, 553–562.
Trajkovic, S., Kolakovic, S., 2009. Evaluation of reference evapotranspiration equations under humid conditions. Water Res. Manage. 23 (14), 3057–3067.
Trajkovic, S., Stojnic, V., 2007. Effect of wind speed on accuracy of Turc method in a humid climate. Facta Univers. Ser.: Archit. Civ. Eng. 5 (2), 107–113.
Turc, L., 1961. Evaluation des besoinsen eau d'irrigation evapotranspiration potentielle. Ann. Agron. 12 (1), 13–49.
UNEP (United Nations Environmental Programme), 1997. World Atlas of Desertification. Editorial commentary by N. Middleton and D.S.G. Edward Arnold, London.
Viswanadham, Y., Silva Filho, V.P., Andre, R.G.B., 1991. The Priestley-Taylor parameter α for the Amazon Forest. Agric. For. Meteor. 38, 211–225.
Wang, S., Lian, J., Peng, Y., Hu, B., Chen, H., 2019. Generalized reference evapotranspiration models with limited climatic data based on random forest and gene expression programming in Guangxi, China. Agirc. Water Manage. 221, 220–230.
Wright, J.L., 1996. Derivation of alfalfa and grass reference evapotranspiration. In: Camp, C.R., Sadler, E.J., Yoder, R.E. (Eds.), Evapotranspiration and irrigation scheduling, Proc., Int. Conf., Irrigation Association and Int. Committee on Irrigation and Drainage. American Society of Agricultural Engineers, St. Joseph, Mich.
Wright, J.L., Jensen, M.E., 1972. Peak water requirements of crops in Southern Idaho. J. Irrig. Drain. Eng. 96 (1), 193–201.
Xiaoying, L., Erda, L., 2005. Performance of the Priestley-Taylor equation in the semiarid climate of North China. Agirc. Water Manage. 71, 1–17.
Xu, C.Y., Chen, D., 2005. Comparison of seven models for estimation of evapotranspiration and groundwater recharge using lysimeter measurement data in Germany. Hydrol. Process. 19, 3717–3734.
Xu, C.Y., Singh, V.P., 2002. Cross comparison of empirical equations for calculating potential evapotranspiration with data from Switzerland. Water Resour. Manage. 16, 197–219.
Xystrakis, F., Matzarakis, A., 2011. Evaluation of 13 empirical reference potential evapotranspiration equations on the island of Crete in Southern Greece. J. Irrig. Drain. Eng. 137 (4), 211–222.
Yoder, R.E., Odhiambo, L.O., Wright, W.C., 2005. Evaluation of methods for estimating daily reference crop evapotranspiration at a site in the humid Southeast United States. Appl. Eng. Agric. 21 (2), 197–202.